Elastic and anelastic properties, vibrational anharmonicity, and fractal bond connectivity of superionic glasses

G. A. Saunders and R. D. Metcalfe*
School of Physics, University of Bath, Bath BA2 7AY, United Kingdom

M. Cutroni, M. Federico, and A. Piccolo
Dipartimento di Fisica, Università di Messina, Contrada Papardo Salita Sperone, 31, 98166 Santa Agata, Messina, Italy
(Received 24 March 1995; revised manuscript received 31 October 1995)

To quantify the thermally activated relaxations of the mobile silver ions in superionic silver phosphosulphate $(Ag_2SO_4)_x(AgPO_3)_{(1-x)}$ and phosphosulphide $(Ag_2S)_x(AgPO_3)_{(1-x)}$ glasses, the broad attenuation peaks reported previously have been analyzed in terms of a Gaussian-type energy distribution. The parameters obtained are used to determine the influence of thermally activated relaxation processes on the temperature dependence of the ultrasonic wave velocity measured between 1.5 and 300 K. After subtraction of the relaxation effects together with those due to anharmonic interactions, another contribution to the temperature dependence of the ultrasonic velocity remains below 100 K, which follows a linear temperature dependence—as predicted by the soft-potential model (SPM) for relaxation of soft harmonic oscillators. The soft HO relaxation contribution to the ultrasonic velocity temperature dependences of silver phosphate-based glasses has a similar magnitude to those determined previously for lanthanide metaphosphate glasses. While the silver phosphate-based glasses have skeletons that are comprised of long chains of phosphate ions, the lanthanide metaphosphate glasses are close to having a three-dimensional structure. The agreement of the excess contribution to the temperature dependence of the ultrasonic velocity with the predictions of the SPM for both types of glass, in spite of their complete differences in structure, is further evidence for the universal applicability of the soft-potential model. To determine the vibrational anharmonicity of the long wavelength acoustic modes in superionic glasses, the hydrostatic pressure derivatives of the second-order elastic stiffness tensor components have been measured for these $(Ag_2SO_4)_x(AgPO_3)_{(1-x)}$, $(Ag_2S)_x(AgPO_3)_{(1-x)}$, vitreous $AgPO_3$ and also for silver iodide molybdate $(AgI)_{0.75}(Ag_2MoO_4)_{0.25}$. To examine further the effects of vibrational anharmonicity, the thermal expansions of the vitreous phosphates have also been measured. The linear thermal expansion coefficient becomes anomalously negative at lower temperatures for the $(Ag_2SO_4)_x(AgPO_3)_{(1-x)}$ and $(Ag_2S)_x(AgPO_3)_{(1-x)}$ glasses. The wide variations found between the elastic and nonlinear acoustic properties of superionic silver phosphate, molybdate, and borate glasses stem from differences in the bonding and connectivities of the glass skeletons.

I. INTRODUCTION

Superionic glasses with high silver ion mobility are important solid electrolytes, finding commercial applications in low-current, long-life batteries. The propagation of ultrasonic waves in superionic materials is strongly influenced by the presence of mobile ions; ultrasonic attenuation and velocity measurements have proved particularly well suited to the study of the dynamics of superionic glasses.[1] A wide ranging ultrasonic study has been made of the elastic and nonlinear acoustic properties of superionic glasses belonging to the silver phosphosulphate $(Ag_2SO_4)_x(AgPO_3)_{(1-x)}$ and silver phosphosulphide $(Ag_2S)_x(AgPO_3)_{(1-x)}$ systems. Contributions to the temperature dependence of the velocity and attenuation of ultrasonic waves arise from anharmonic effects and thermally activated relaxation processes. Physical properties, such as ultrasonic attenuation or thermal expansion, which depend upon ionic thermal motion, are dominated by vibrational anharmonicity. The anharmonicity of the long-wavelength acoustic modes can be determined from the effects of pressure on the elastic moduli. Since there is no quantitative information available on the anharmonicity of the long-wavelength acoustic modes for glasses belonging to the systems silver phosphosulphate $(Ag_2SO_4)_x(AgPO_3)_{(1-x)}$, silver phosphosulphide $(Ag_2S)_x(AgPO_3)_{(1-x)}$, or silver iodide molybdate $(AgI)_x(Ag_2MoO_4)_{(1-x)}$, measurements have now been made of the hydrostatic pressure derivatives of the second-order elastic stiffness tensor components for glasses of each of these types. To extend knowledge of the vibrational anharmonicity, the thermal expansions of the silver phosphosulphates and phosphosulphides have also been measured.

High-pressure ultrasonic studies have been made previously for other types of superionic glasses: $(Ag_2O)_y(B_2O_3)_{(1-y)}$, $(AgI)_x\{(Ag_2O)_y(B_2O_3)_{(1-y)}\}_{(1-x)}$ (Ref. 2), and $(AgI)_x(AgPO_3)_{(1-x)}$ (Ref. 3) glasses. For the borate glasses it was found that, while the anharmonicity of the longitudinal mode is normal, $(\partial C^S_{11}/\partial P)_{T,P=0}$ is positive and that for the shear wave it is to a degree anomalous in that $(\partial C^S_{44}/\partial P)_{T,P=0}$ is negative: The shear mode softens under pressure.[2] By contrast, the vibrational anharmonicities of both the long-wavelength shear and longitudinal modes propagated in $(AgI)_x(AgPO_3)_{(1-x)}$ glasses are normal.[3] Furthermore, the values of the acoustic mode Grüneisen parameters of the glasses in these two superionic systems have established that the pressure dependences of the long-

wavelength acoustic vibrational mode energies are quite different. The structures of silver borates and phosphates are different in kind. Borate glasses consist primarily of planar units, (BO_3) triangles and hexagonal (B_3O_3) rings[4,5] and so are probably comprised of two-dimensional networks, while phosphate glasses are based on linear chains of PO_4 tetrahedra. In these circumstances their elastic and nonlinear acoustic properties might be expected to differ markedly. It has been with this in mind in particular that ultrasonic studies as a function of pressure have been made of the $(Ag_2SO_4)_x(AgPO_3)_{(1-x)}$ and $(Ag_2S)_x(AgPO_3)_{(1-x)}$ glasses and also for a glass $(AgI)_{0.75}(Ag_2MoO_4)_{0.25}$ containing (MoO_4) tetrahedra. For the silver phosphate glasses, substitution of sulphur for oxygen increases the cationic conductivity. Electrical conductivity and ultrasonic attenuation studies[6] have shown that the behavior of $(Ag_2S)_x(AgPO_3)_{(1-x)}$ glasses occupies an intermediate position between that of AgI-doped and network-modified glasses. A suggestion that the sulphide can act both as an interstitial dopant and as a network modifier has been confirmed by ^{31}P NMR magic angle spinning spectroscopy.[6] A similar study[7] of $(Ag_2SO_4)_x(AgPO_3)_{(1-x)}$ glasses has shown that for compositions with $x<0.2$ the sulphate SO_4^{2-} ion acts as a network modifier, preferentially occupying a bridging position between two end units. The fractal bond connectivity[8,3] is used here to provide physical insight into the way in which structural differences, which dominate the ionic behavior of the different superionic glasses, influence their elastic and nonlinear acoustic properties.

Anomalies in a wide range of physical properties at low temperatures due to frozen-in supplementary degrees of freedom are a characteristic feature of glasses.[9,10] Measurements made in the temperature range 1.2–40 K on the ionic conducting $(AgI)_x(Ag_2O{\cdot}B_2O_3)_{(1-x)}$ glasses with $x=0$, 0.2, 0.5, and 0.65 have shown that there is an additional specific heat C, over that predicted from the Debye theory, which is associated with the excess of localized vibrational states.[11] A pronounced maximum occurs in the plot of $C(T)/T^3$ with temperature T. Theoretical models, which have been proposed to account for the universal form of the excess of density of vibrational states in glasses, include (i) a possible fractal structure[12,13] and (ii) soft harmonic potentials with a random distribution of coupling constants.[14,15] The anomalous specific heat of the $(AgI)_x(Ag_2O{\cdot}B_2O_3)_{(1-x)}$ glasses was analyzed in terms of an energy spectrum comprised schematically of long-wavelength phonons and short-wavelength, localized modes with a fractal nature.[11] The crossover frequency ω_{CO} from a regime of phonons to modes localized on clusters of low effective fractal dimensionality corresponded to a characteristic length L of about 30 Å in these glasses, in accordance with that predicted by the phonon-fracton model. In general, the parameters found from the model for a fracton-phonon density-of-states fit to the excess specific heat have the same magnitudes as those found for other amorphous materials, including a number of phosphate glasses.[16] Although the model can be used to fit the data, such an approach leaves out of consideration the questionable fractality of glasses. In principle, the universal complex of anomalous thermal, acoustic, and optical vibrational properties of glasses can also be accounted for phenomenologically within the framework of the soft-potential model (SPM). One prediction of the SPM is the occurrence in the temperature dependence of $C(T)/T^3$ of a minimum at a temperature T_{min} at which crossover takes place between harmonic and anharmonic states from a $C\sim T$ to $C\sim T^5$ behavior. Inspection of the specific-heat results obtained for the $(AgI)_x(Ag_2O{\cdot}B_2O_3)_{1-x}$ glasses [see Fig. 1(a) of Ref. 11] shows that these ionic glasses do show a minimum in $C(T)/T^3$ at $T_{min}\sim 2.5$ K. Recently, it has been found[17] for $(La_2O_3)_{0.25}(P_2O_5)_{0.75}$ and $(Sm_2O_3)_{0.25}(P_2O_5)_{0.75}$ metaphosphate glasses that after the subtraction of relaxation and anharmonic contributions, a contribution to the ultrasonic wave velocity temperature dependence remains that has linear temperature dependence in accordance with a prediction of the soft-potential model for the relaxation of soft harmonic oscillators.[18–20] Lanthanide metaphosphate glasses have quite different structures from the superionic silver phosphate glasses. However, if, as suggested,[18–20] the SPM, which is an extension of the tunneling model for two-level systems (TLS's), can account for the ''universality'' of the low-temperature physical properties of glasses, then a contribution from the relaxation of soft harmonic oscillators would also be expected in the ultrasonic wave velocity in the silver phosphate glasses. Hence finding out if such a contribution exists in superionic silver phosphosulphate $(Ag_2SO_4)_x(AgPO_3)_{(1-x)}$ and silver phosphosulphide $(Ag_2S)_x(AgPO_3)_{(1-x)}$ glasses is an essential requirement for developing an understanding of the mechanisms which regulate the ultrasound wave propagation in these glasses.

II. EXPERIMENTAL DETAILS

These silver phosphosulphate and phosphosulphide glasses have been studied previously by a variety of techniques including conductivity, acoustic attenuation, and NMR.[6,7] For the ultrasonic work silver phosphosulphate and phosphosulphide glasses of formula $(Ag_2SO_4)_x(AgPO_3)_{(1-x)}$ and $(Ag_2S)_x(AgPO_3)_{(1-x)}$, with x ranging between 0.1 and 0.3, and a sample of a pure silver phosphate glass ($x=0$) were prepared in the form of cylinders of diameter and length around 5 mm. The molybdate $(AgI)_x(Ag_2MoO_4)_{(1-x)}$ glass was prepared by melting together AgI and Ag_2MoO_4 in a 3:1 mole ratio in a Pyrex tube. It was the same material as that used to assess ion hopping properties by measurements of the ac conductivity, the dependence on temperature of the attenuation of longitudinal ultrasonic waves and shear wave velocity, and thermal expansion.[21]

To make ultrasonic wave velocity and attenuation measurements, samples were cut and polished to have flat and parallel faces to within 10^{-3} rad. Parallelism of the faces was examined using an optical interference method and ensured to within one wavelength of sodium light. Quartz transducers (X cut for longitudinal, Y cut for shear waves), driven at their fundamental frequency of 10 MHz, were bonded to the specimens using Nonaq stopcock grease as the bonding agent between samples and transducers. Dow resin 276-V9 was used as the bonding material above room temperature.

The ultrasonic wave velocities were measured using the pulse echo overlap technique,[22] which, having a sensitivity of better than 1 part in 10^5, is particularly suited for measuring the rather small changes in ultrasonic wave velocity induced by changing the temperature or by application of pres-

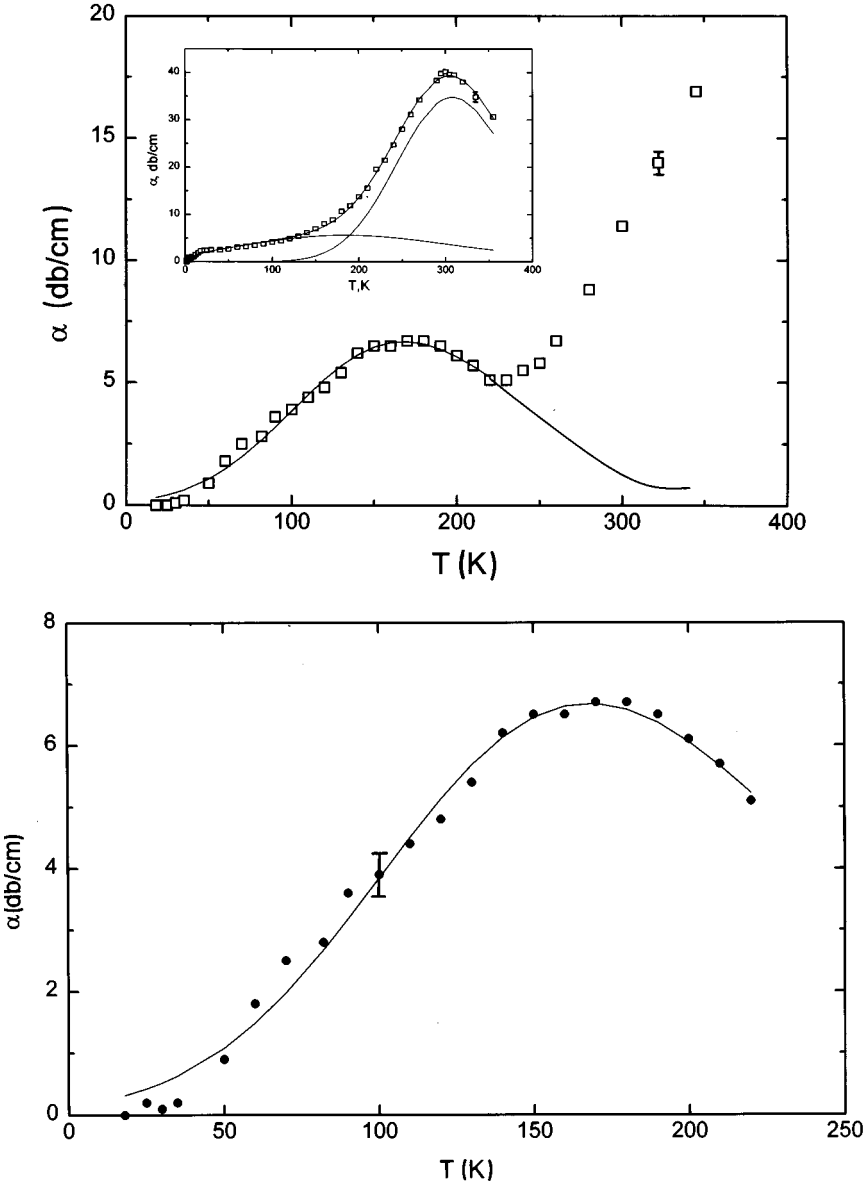

FIG. 1. Comparison between the experimentally determined attenuation of 30 MHz ultrasonic waves propagated in $(Ag_2SO_4)_{0.3}(AgPO_3)_{0.7}$glass as a function of temperature and that determined from a theoretical fit (solid line) to the relaxation model [Eqs. (1) and (2)] using a distribution of activation energies [Eq. (3)]. The inset shows the acoustic absorption as a function of temperature in the $(Ag_2S)_{0.3}(AgPO_3)_{0.7}$ glass at 30 MHz. Solid lines represent the best fit and show the two relaxational contributions described in the text.

sure. Hydrostatic pressure up to 0.15 GPa was applied in a piston-and-cylinder apparatus using silicone oil as the pressure-transmitting medium. The pressure was determined from the change in resistance of a precalibrated manganin wire coil in the pressure cell. To circumvent the requirement of the determination of pressure-induced changes in sample dimensions, the ''natural velocity'' W approach[23] was used. The stress dependences of the relative changes in natural velocities of both longitudinal and shear ultrasonic waves were found to be linear up to the maximum pressure applied. Hence the slope of the experimental results for the dependence of the natural wave velocity upon pressure could be used to determine the hydrostatic pressure derivatives $(\partial C^S_{11}/\partial P)_{T,P=0}$ of the elastic stiffnesses.

III. ULTRASONIC ATTENUATION

In general, the ultrasonic attenuation of $(Ag_2S)_x(Ag_2PO_3)_{(1-x)}$ glasses, which has been described and discussed in detail in Ref. 6, is quite similar to that of the

TABLE I. Values computed from the best fits of the relaxation model equations (1)–(3) to the experimental ultrasonic data for the most probable activation energy E_m, relaxation time τ, and width E_0 of the energy distribution $P(E)$ in superionic glasses.

	E_{m1} (eV)	E_{01} (eV)	τ_1 (10^{-10} s)	E_{m2} (eV)	E_{02} (eV)	τ_2 (10^{-14} s)	θ_D (K)	V_L (m s^{-1})	V_S (m s^{-1})
$(Ag_2S)_{0.3}(AgPO_3)_{0.7}$	0.4	0.08	7.0	0.138	0.088	9.8	192	3337	1510
$(Ag_2SO_4)_{0.3}(AgPO_3)_{0.7}$				0.094	0.033	0.99	179	3317	1376

$(Ag_2I)_x(AgPO_3)_{(1-x)}$ glasses; at temperatures T below 10 K, it is characterized by a plateau[6] of the type attributed to phonon-assisted relaxation or TLS's predicted by Jäckle:[24] The acoustic wave interacts with the TLS's and modifies their thermal equilibrium population so that a new equilibrium distribution is attained with the cooperation of the thermal phonons. Above 10 K the acoustic absorption is dominated by a broad loss peak, characteristic of glasses,[25] which was analyzed[6] assuming the existence of two thermally activated relaxation processes. The relaxation parameters obtained from a best fit indicate that the intermediate-temperature region is characterized by an activation energy of about 0.1 eV whose value depends on the salt content. The same activation energy value has recently been obtained from the Arrhenius fit of the microwave conductivity[26] on glasses with the same composition and has been analyzed in terms of unsuccessful ion hopping. The high-temperature–low-frequency region, where the ionic diffusion is dominant, is characterized by a higher activation energy (about 0.4 eV) corresponding to the σ_{dc} energy value.

The ultrasonic attenuation of the $(Ag_2SO_4)_{0.1}(AgPO_3)_{0.9}$ glass, which was measured by Scotti *et al.*,[7] does not show well-defined relaxation effects due to the ionic diffusion. However, in the low-temperature region ($T<10$ K), the acoustic attenuation, like the velocity (see below), shows typical TLS effects. For the glasses with higher Ag_2SO_4 content of compositions $(Ag_2SO_4)_{0.2}(AgPO_3)_{0.8}$ and $(Ag_2SO_4)_{0.3}(AgPO_3)_{0.7}$ in the region above 10 K, the longitudinal absorption shows a small peak on a continuously increasing background as the temperature rises.[7] The broad intermediate-temperature relaxation loss peak is also superimposed on this background, although at a rather higher temperature than that observed for the $(Ag_2S)_x(AgPO_3)_{(1-x)}$ glasses.[6] To obtain the relaxation parameters (needed to analyze the ultrasonic velocity data, which is reported here), the acoustic attenuation $\alpha(\omega,T)$ accruing from relaxation processes has been described by[1,6,7]

$$\alpha_l(\omega,T)=\frac{\Delta_l}{2V}\int P_l(E)\,\frac{\omega^2\tau_l(E)}{1+\omega^2\tau_l^2(E)}\,dE, \tag{1}$$

where Δ is the relaxation strength, V and ω are the velocity and angular frequency of the inserted ultrasonic wave, and the subscript $l=2$ identifies the parameters pertaining to the low-energy motion, while $l=1$ identifies those for ionic diffusion. Normal practice is to express the relaxation time τ for the absorbing processes by an Arrhenius-type relationship

$$\tau=\tau_0\exp(E/kT). \tag{2}$$

Here τ_0 is a characteristic time and E is the mean activation energy. In this phenomenological model a Gaussian distribution is assumed for the distribution $P(E)$:

$$P(E)=\frac{1}{(2\pi E_0)^{1/2}}\exp\left(-\frac{(E-E_m)^2}{2E_0^2}\right), \tag{3}$$

with E_m being the most probable value and E_0 the width of the distribution. A typical fit to the experimental attenuation of ultrasonic waves with a driving ultrasonic frequency of 30 MHz obtained for the $(Ag_2SO_4)_{0.3}(AgPO_3)_{0.7}$ glass is shown in Fig. 1 as an example; the corresponding computed relaxation parameters are given in Table I, together with those determined for the $(Ag_2S)_{0.3}(AgPO_3)_{0.7}$ glass from an analysis of the ultrasonic data given in Ref. 6. In general, the temperature dependences of the acoustic properties in the MHz frequency region shows that the Ag_2S and Ag_2SO_4 dopant salts play a different role in the structure-dependent properties of these superionic glasses.[6,7]

IV. ULTRASONIC WAVE VELOCITY AND ELASTIC STIFFNESS TENSOR COMPONENTS

The ultrasonic wave velocities, the second-order elastic stiffness tensor components C_{11} and C_{44}, and the bulk modulus B_0^S calculated at room temperature from the ultrasonic wave velocity measurements for $(Ag_2SO_4)_x(AgPO_3)_{(1-x)}$, $(Ag_2S)_x(AgPO_3)_{(1-x)}$, and $(AgI)_{0.75}(Ag_2MoO_4)_{0.25}$ are compared with the elastic properties of other superionic glasses in Table II. The pure $AgPO_3$ phosphate glass is rather less stiff, and the temperature derivatives of the stiffnesses are slightly larger than for the doped samples. In general, the Ag_2S modifier has a greater effect on elastic properties than Ag_2SO_4. For the $(Ag_2SO_4)_x(AgPO_3)_{(1-x)}$ and $(Ag_2S)_x(AgPO_3)_{(1-x)}$ systems, increasing the (Ag_2SO_4) or (Ag_2S) content from x equal to 0.1–0.3 increases the longitudinal and shear velocity (and hence the elastic stiffnesses). The velocities of ultrasonic waves in the molybdate glass are much slower than those in the silver phosphates and borates, and the elastic stiffnesses C_{11} and C_{44} and the bulk modulus B_0^S are correspondingly much smaller: The interatomic binding in the molybdate glass is much weaker.

The temperature dependences of the velocities of longitudinal and shear 10 MHz ultrasonic waves propagated in $(Ag_2S)_x(AgPO_3)_{(1-x)}$ glasses with x equal to 0.1, 0.2, and 0.3 are shown in Fig. 2 and for the corresponding $(Ag_2SO_4)_x(AgPO_3)_{(1-x)}$ glasses in Fig. 3. As would be expected for vitreous materials, the temperature dependences of the ultrasonic wave velocities of these glasses do not conform with the behavior usually observed in crystalline materials for the effects of vibrational anharmonicity, namely, a linear increase of the ultrasonic wave velocity with decreasing temperature, terminating in a zero slope at low temperatures. As the temperature is reduced, the ultrasonic wave velocities continue to increase (Figs. 2 and 3). Such behavior is associated with the interaction of the ultrasonic waves with TLS's through a thermally activated, structural relaxation process. Recently, it has been found[17] for the case of the lanthanum $(La_2O_3)_{0.25}(P_2O_5)_{0.75}$ and samarium $(Sm_2O_3)_{0.25}(P_2O_5)_{0.75}$ metaphosphate glasses that below about 100 K the temperature dependence of the ultrasonic wave velocity, after subtraction of the relaxation and anharmonic contributions, follows a linear law as predicted[20] by the SPM (Refs. 14, 15, 17–20) for the relaxation of soft harmonic oscillators. Encouraging agreement was found between the parameters regulating this mechanism and those determined from acoustic attenuation results. The next step is to find out if the SPM prediction holds for the superionic glasses of present interest. To do this, it is necessary to extract the anharmonic and relaxation contributions.

The anharmonic effects have been determined by using an extension to isotropic materials[27] of the quasiharmonic continuum model,[28] writing the temperature dependence of the

TABLE II. Elastic and nonlinear acoustic properties of $(Ag_2SO_4)_x(AgPO_3)_{(1-x)}$ $(Ag_2S)_x(AgPO_3)_{(1-x)}$, and $(AgI)_x(Ag_2MO_4)_{1-x}$, glasses at room temperature 296 K compared with data for $(AgI)_x((Ag_2O)_{0.33}(B_2O_3)_{0.67})_{(1-x)}$, $(Ag_2O)_x(B_2O_3)_{(1-x)}$ (Ref. 2), and $(AgI)_x(AgPO_3)_{(1-x)}$ (Ref. 3) glasses.

	Mole Fraction	Density	Ultrasonic wave velocity ($m\ s^{-1}$)		Elastic moduli ($\times 10^{10}\ N\ m^{-2}$)			Bond connectivity	Hydrostatic pressure derivative of elastic stiffness			Acoustic mode	Gruneiser parameters		Debye temperature
	x	($kg\ m^{-3}$)	V_L	V_S	C_{11}	C_{44}	B	d	C'_{11}	C'_{44}	B'	γ_l	γ_t	γ_{el}	Θ_D
Sample															
$AgPO_3$ (pure)	0	4470	3040	1420	4.14	0.896	2.95	1.22	7.59	0.63	6.75	2.53	0.87	1.42	198
$(Ag_2SO_4)_x(AgPO_3)_{(1-x)}$	0.1	4520	3180	1350	4.56	0.829	3.45	0.96	7.22	0.59	6.43	2.57	1.07	1.57	189
	0.3	4890	2900	1210	4.11	0.718	3.15	0.91	8.07	0.59	7.28	2.93	1.13	1.73	171
$(Ag_2S)_x(AgPO_3)_{(1-x)}$	0.1	4940	3140	1390	4.86	0.951	3.59	1.11	7.56	0.78	6.52	2.63	1.31	1.75	196
	0.3	5100	2990	1340	4.56	0.920	3.34	1.10	6.39	0.86	5.24	2.17	1.40	1.66	182
$(Ag_2O)_x(B_2O_3)_{(1-x)}$	0.09	2520	3753	2074	3.552	1.085	2.105	2.03	3.30	−0.21	3.68	0.84	−0.37	0.03	296
	0.11	2590	3761	2105	3.659	1.146	2.131	2.15	3.40	−0.19	3.60	0.80	−0.34	0.04	298
	0.14	2850	3973	2167	4.497	1.338	2.632	2.03	3.60	−0.21	3.89	0.91	−0.38	0.05	310
	0.20	3280	4191	2236	5.761	1.640	3.575	1.84	4.06	−0.29	4.45	1.10	−0.49	0.04	322
	0.33	4030	4232	2181	7.218	1.917	4.661	1.64	3.88	−0.15	4.08	1.09	−0.34	0.13	311
$(AgI)_x(AgPO_3)_{(1-x)}$	0	4449	3350	1490	4.99	0.992	3.67	1.10	8.47	0.73	7.50	2.95	1.18	1.77	208
	0.11	4675	3160	1390	4.67	0.902	3.47	1.04	9.60	0.89	8.41	3.40	1.54	2.16	191
	0.21	4852	2970	1300	4.29	0.826	3.19	1.04	9.68	0.88	8.51	3.43	1.53	2.16	176
	0.31	5048	2810	1220	3.99	0.751	2.99	1.01	9.37	0.85	8.24	3.34	1.52	2.13	162
	0.39	5263	2660	1130	3.72	0.677	2.82	0.96	9.73	0.78	8.69	3.52	1.46	2.14	149
$(AgI)_x((Ag_2O)_{33}(B_2O_3)_{0.7})_{(1-x)}$	0	4030	4232	2181	7.218	1.917	4.66	1.64	3.88	−0.15	4.08	1.09	−0.34	0.13	311
	0.1	4270	4079	2078	7.105	1.844	4.64	1.59	3.40	−0.019	3.43	0.95	−0.19	0.19	288
	0.2	4380	3895	2049	6.645	1.839	4.19	1.76	5.18	−0.047	5.24	1.47	−0.22	0.34	273
	0.6	4840	3011	1603	4.388	1.244	2.73	1.82	6.89	−0.22	7.18	1.98	−0.40	0.39	227
$(AgI)_{0.2}(Ag_2O)_{0.2}$ $(B_2O_3)_{0.8}$	0.2	3360	3911	2141	5.139	1.540	3.08	2.00	4.30	−1.25	5.96	1.16	−1.42	−0.57	276
$(AgI)_x(Ag_2MoO_4)_{1-x}$	0.75	6211	1941	789	2.34	0.387	1.82	0.85	7.79	0.51	7.11	2.86	1.03	1.64	

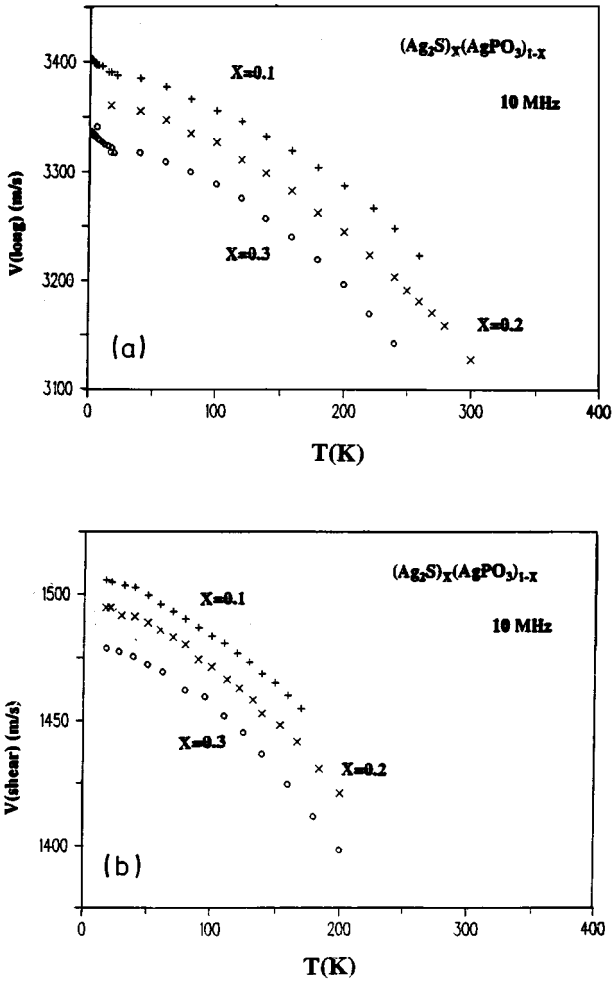

FIG. 2. Temperature dependence of the velocity of (a) longitudinal and (b) shear 10 MHz ultrasonic waves propagated in phosphosulphide $(Ag_2S)_x(AgPO_3)_{(1-x)}$ glasses.

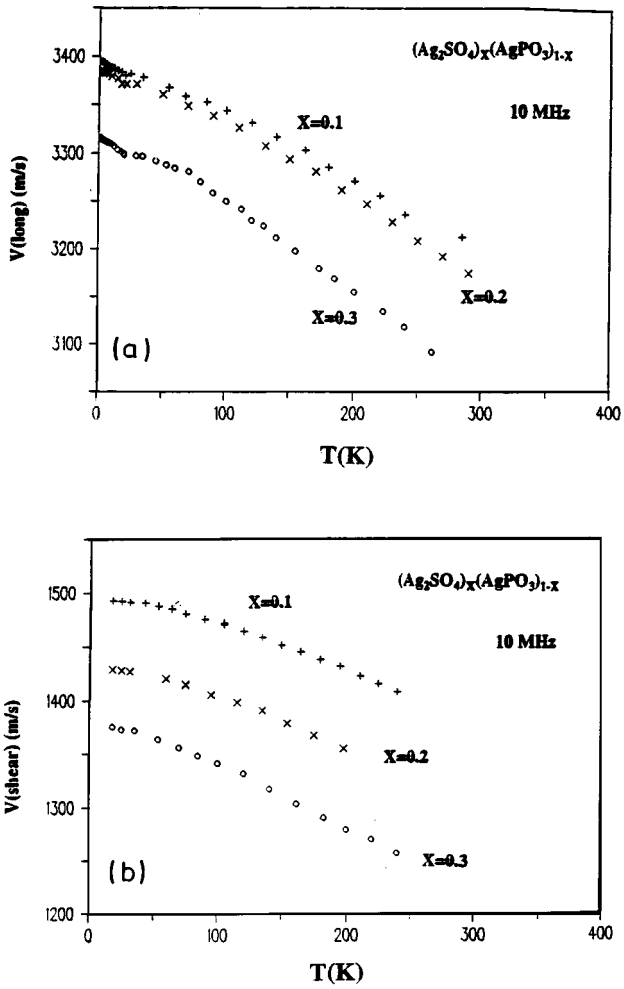

FIG. 3. Temperature dependence of the velocity of (a) longitudinal and (b) shear 10 MHz ultrasonic waves propagated in $(Ag_2SO_4)_x(AgPO_3)_{(1-x)}$ glasses.

longitudinal ultrasonic wave velocity as

$$V_L = V_{L_0}\left[\frac{L}{L_0}\right]^{3/2}\left[1-\Gamma_L F\left(\frac{T}{\theta}\right)\right]^{1/2}, \tag{4}$$

where

$$F\left[\frac{T}{\theta}\right]=\left[3\left(\frac{T}{\theta}\right)^4\int_0^{\theta/T}\frac{x^3\,dx}{e^x-1}\right]. \tag{5}$$

Here V_{L_0} is the ultrasonic wave velocity at $T=0$ K, L is the specimen length, and θ is the Debye temperature. The coefficient Γ_L, which depends upon the Grüneisen parameter, has been selected to fit the velocity measured at high temperatures where any effects of the relaxation processes are negligible. The calculated relative temperature dependences in the anharmonic contribution to the ultrasonic wave velocity with temperature for the $(Ag_2SO_4)_{0.3}(AgPO_3)_{0.7}$ and $(Ag_2S)_{0.3}(AgPO_3)_{0.7}$ glasses are shown in Fig. 4.

The dispersion arising from the thermally activated relaxations of the structural defects has been calculated using[29]

$$\left[\frac{\Delta V}{V_0}\right]_{\rm rel}=-\frac{B_i^2}{8\rho V_1^2 k_B T}\int P(E)\,\frac{1}{1+\omega^2\tau^2(E)}\,dE \tag{6}$$

from the parameters given in Table I determined from the acoustic attenuation peak (Fig. 1). The results calculated for the $(Ag_2SO_4)_{0.3}(AgPO_3)_{0.7}$ and the $(Ag_2S)_{0.3}(AgPO_3)_{0.7}$ glasses are shown in Fig. 4.

When the sum of the anharmonic and relaxation contributions is subtracted from the experimentally determined velocity of longitudinal ultrasonic waves as a function of temperature, an excess term in $\Delta V/V_0$, which follows a linear temperature dependence, remains, evidencing a contribution from another mechanism to the temperature dependence of the velocity in this temperature range. In the case of the lanthanide phosphate glasses, it was shown that, on the basis of the SPM approach, the excess velocity contribution derives dominantly from a relaxation mechanism involving soft single-well harmonic oscillators (HO's), which interact with the ultrasonic deformation field by a modulation of the interlevel spacing.[17] This mechanism leads to the following contribution to the sound velocity in the terminology detailed in Ref. 20:

$$\left[\frac{\delta V}{V}\right]_{\rm HO}=-\frac{28.2^{1/2}}{9}\,C_i\,\frac{k}{E_0}\,(T-T_0). \tag{7}$$

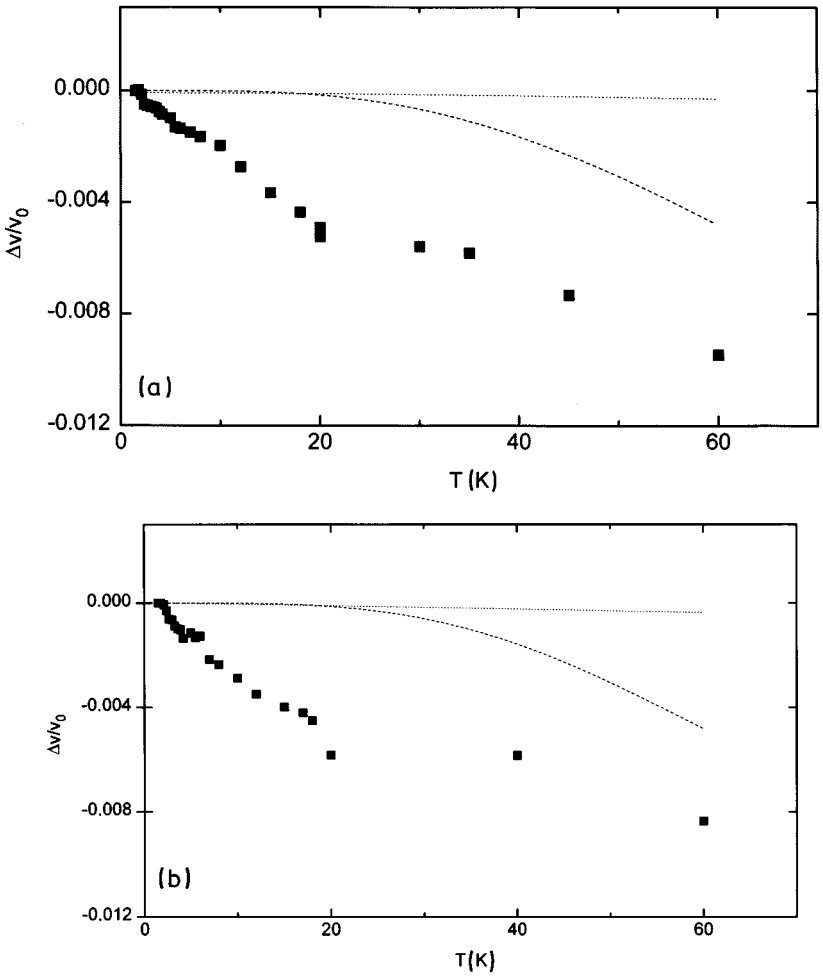

FIG. 4. Temperature dependence of the experimental fractional ultrasound velocity $\Delta V/V_0$ (solid squares) for (a) $(Ag_2SO_4)_{0.3}(AgPO_3)_{0.7}$ and (b) $(Ag_2S)_{0.3}(AgPO_3)_{0.7}$ glasses. The anharmonic (dashed line) and relaxation (dotted line) contributions to $\Delta V/V_0$ have been calculated using Eqs. (4) and (6), respectively.

The linear dependence of the excess velocity contribution found here at low temperature for the $(Ag_2SO_4)_{0.3}(AgPO_3)_{0.7}$ and $(Ag_2S)_{0.3}(AgPO_3)_{0.7}$ ionic glasses (Fig. 5) is in accordance with this SPM prediction. The slopes b (Fig. 5) are very similar to those found for the lanthanum $(La_2O_3)_{0.25}(P_2O_5)_{0.75}$ and samarium $(Sm_2O_3)_{0.25}(P_2O_5)_{0.75}$ metaphosphate glasses, which were 2.62×10^{-4} and 1.91×10^{-4}, respectively. Although the silver phosphate-based and lanthanide metaphosphate glasses have quite different structures, the soft HO relaxation contribution to their ultrasonic velocity temperature dependences is of similar magnitude, a finding again in accordance with the suggestion that the SPM should be universally applicable to glasses.

The temperature dependences of the elastic stiffnesses are

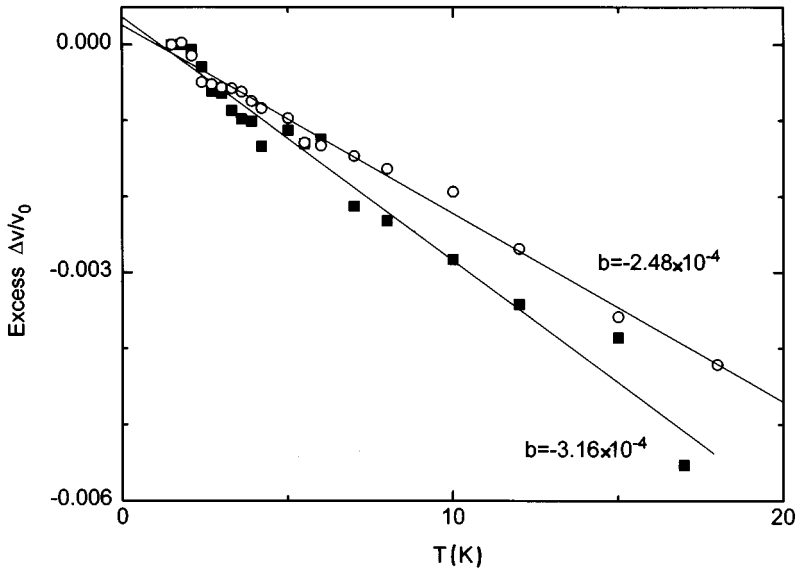

FIG. 5. Contribution from a relaxation mechanism involving soft single-well harmonic oscillators (HO's) to the fractional longitudinal ultrasound velocity in excess of that provided by the sum of the anharmonic and relaxation terms for $(Ag_2SO_4)_{0.3}(AgPO_3)_{0.7}$ (circles) and $(Ag_2S)_{0.3}(AgPO_3)_{0.7}$ (solid squares) glasses.

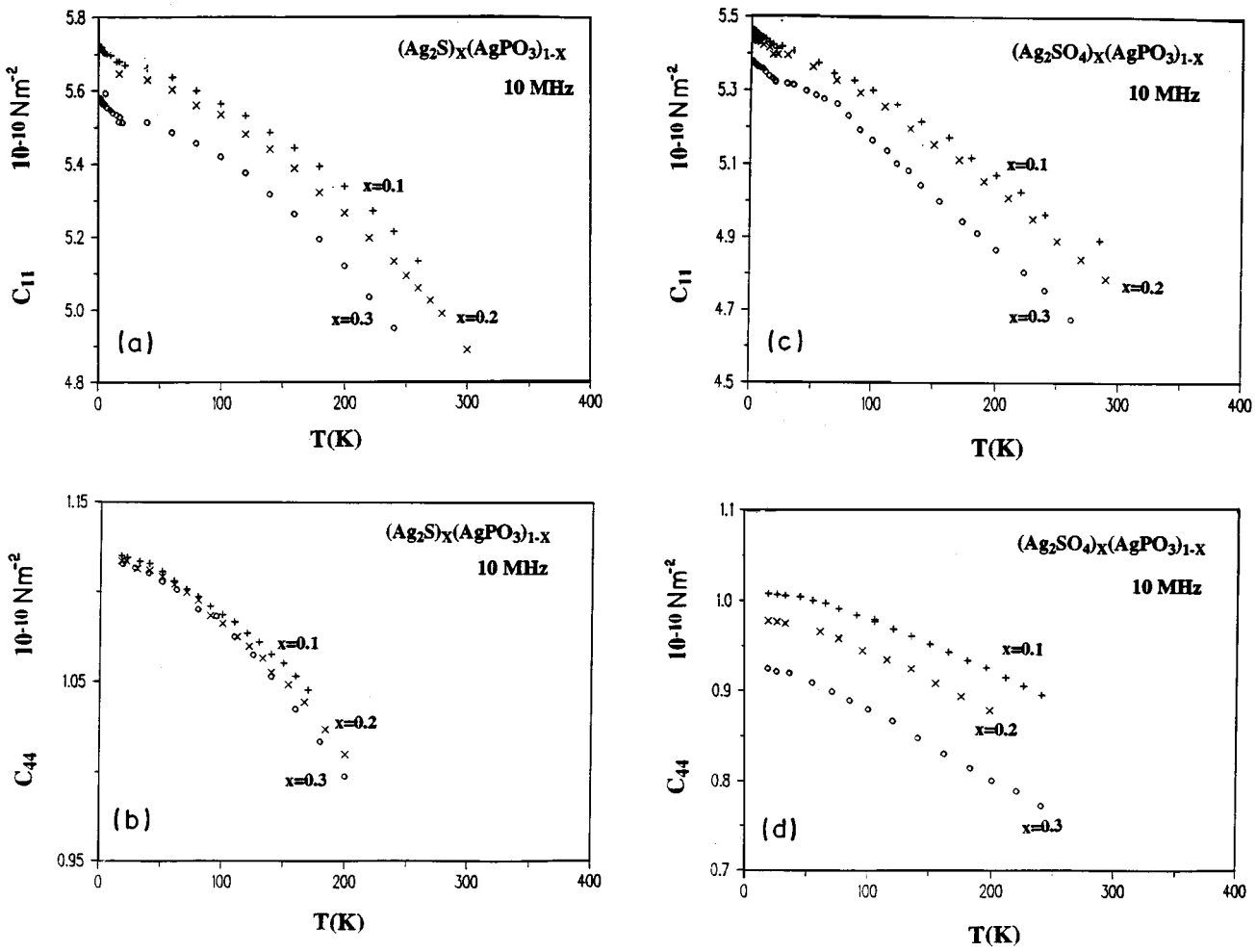

FIG. 6. Temperature dependence of the elastic stiffnesses C_{11} and C_{44} (a) and (b) in $(Ag_2S)_x(AgPO_3)_{(1-x)}$ and (c) and (d) $(Ag_2SO_4)_x(AgPO_3)_{(1-x)}$ glasses.

shown in Fig. 6; at high temperatures, both the longitudinal C_{11} and shear C_{44} stiffnesses increase approximately linearly with decreasing temperature and at lower temperatures begin to flatten out; this is the usual behavior expected from the conventional model for vibrational anharmonicity. This linear behavior has been confirmed by measurements of the temperature dependence of the longitudinal elastic constant for the pure $AgPO_3$ glass and for two compositions of vitreous $(Ag_2SO_4)_x(AgPO_3)_{(1-x)}$ in the range 293–393 K, below the glass-forming range (430–510 K). However, at low temperatures the behavior of the longitudinal modulus C_{11} for both these types of superionic glasses deviates from that expected from anharmonic model, showing a continuous increase associated with the relaxation mechanism involving soft single-well harmonic oscillators.

V. EFFECTS OF HYDROSTATIC PRESSURE ON THE ELASTIC MODULI

The relative changes in the natural velocities of longitudinal and shear ultrasonic waves propagated in the $(Ag_2S)_x(AgPO_3)_{(1-x)}$ and $(Ag_2SO_4)_x(AgPO_3)_{(1-x)}$ glasses were found to be linearly dependent upon hydrostatic pressure (Figs. 7 and 8); this was also true for the $(AgI)_{0.75}(Ag_2MoO_4)_{0.25}$ glass. The hydrostatic pressure derivatives of the longitudinal $(\partial C_{11}^S/\partial P)_{T,P=0}$ and shear $(\partial C_{44}^S/\partial P)_{T,P=0}$ elastic stiffnesses are compared with those of other superionic glasses in Table II. The pressure derivatives for $(Ag_2SO_4)_x(AgPO_3)_{(1-x)}$, $(Ag_2S)_x(AgPO_3)_{(1-x)}$, and $(AgI)_{0.75}(Ag_2MoO_4)_{0.25}$ glasses show normal behavior in that $(\partial C_{11}^S/\partial P)_{T,P=0}$ is much larger than $(\partial C_{44}^S/\partial P)_{T,P=0}$ and both are positive. Thus the effects of hydrostatic pressure on the elastic properties of these glasses resemble those found[3] for the $(AgI)_x(AgPO_3)_{(1-x)}$ glasses. By contrast, in the case of the $(Ag_2O)_y(B_2O_3)_{(1-y)}$ and $(AgI)_x\{(Ag_2O)_y(B_2O_3)_{(1-y)}\}_{(1-x)}$ glasses the shear stiffness pressure derivative $(\partial C_{44}^S/\partial P)_{T,P=0}$ has an anomalous negative value.[2]

A negative $(\partial C_{IJ}^S/\partial P)_{T,P=0}$ signifies that application of pressure produces an anomalous decrease of the vibrational frequencies ω_i associated with long-wavelength acoustic modes. This can be quantified by considering the mode Grüneisen parameters

$$\gamma_i = -\partial \ln\omega_i / \partial \ln V, \tag{8}$$

which express the volume (or strain) dependence of the normal mode frequency ω_i. For an isotropic solid there are just two Grüneisen parameters, namely, γ_L and γ_S for longitudi-

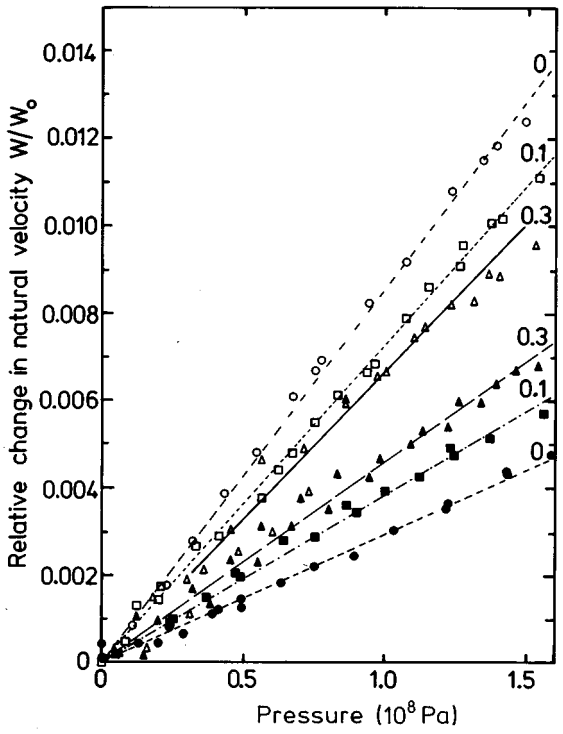

FIG. 7. Hydrostatic-pressure-induced relative change in the natural velocity of longitudinal (upper three plots) and shear (lower three plots) ultrasonic waves propagated in $(Ag_2S)_x(AgPO_3)_{(1-x)}$ glasses.

nal and shear elastic waves, respectively. These have been obtained from the elastic constants and their hydrostatic pressure derivatives using

$$\gamma_1 = -\frac{B^S}{6C_{11}}\left[3-\frac{2C_{12}}{B^S}-3\left(\frac{\partial B}{\partial P}\right)-4\left(\frac{\partial C_{44}}{\partial P}\right)\right], \quad (9)$$

$$\gamma_s = -\frac{1}{6C_{44}}\left[2C_{44}-3B^S\left(\frac{\partial C_{44}}{\partial P}\right)-\frac{3B^S}{2}+\frac{3C_{12}}{2}\right]. \quad (10)$$

The mean long-wavelength acoustic mode Grüneisen parameter γ_{el} is then given by

$$\gamma_{el}=\{(\gamma_L/V_L^3)+(2\gamma_S/V_S^3)\}/\{(1/V_L^3)+(2/V_S^3)\}. \quad (11)$$

The similarities between the Grüneisen parameters, given in Table II, for the $(AgI)_x(AgPO_3)_{(1-x)}$, $(Ag_2SO_4)_x(AgPO_3)_{(1-x)}$, $(Ag_2S)_x(AgPO_3)_{(1-x)}$, and pure $AgPO_3$ glasses show that the acoustic mode vibrational anharmonicities are similar in magnitude in each of these phosphate glasses, each of which have a fractal bond connectivity of about unity (Sec. VII). The mode frequencies increase in the usual manner under pressure, the effect being larger for the volume-dependent longitudinal modes. These results are in marked contrast to the Grüneisen parameters obtained for the $(Ag_2O)_y(B_2O_3)_{(1-y)}$ and $(AgI)_x\{(Ag_2O)_y(B_2O_3)_{(1-y)}\}_{(1-x)}$ glasses for which the longitudinal mode parameter γ_L is substantially smaller and that γ_S for the shear mode is negative.[2]

It is common practice to use ultrasonic velocity data to extrapolate the compression $V(P)/V_0$ of a material up to high pressures by recourse to an equation of state, for example, that due to Murnaghan,[30] which is widely used,

$$P=\left(\frac{B_0^T}{B_0'}\right)\left[\left(\frac{V_0}{V}\right)^{B_0'}-1\right], \quad (12)$$

which in logarithmic form is

$$\ln\left(\frac{V_0}{V}\right)=\frac{1}{B_0'}\ln\left[\frac{B_0'P}{B_0^T}+1\right]. \quad (13)$$

Here B_0^T is the isothermal bulk modulus and B_0' is equal to $(\partial B_0^T/\partial P)_{P=0}$. This has been used to determine the compressions $V(P)/V_0$ of the $(Ag_2SO_4)_x(AgPO_3)_{(1-x)}$ and $(Ag_2S)_x(AgPO_3)_{(1-x)}$ glasses. Since the elastic moduli of the molybdate $(AgI)_{0.25}(Ag_2MoO_4)_{0.75}$ glass (Table II) are comparatively small, this glass has a much larger compression than found for the stiffer phosphates (Fig. 9).

VI. THERMAL EXPANSION

The temperature dependences of changes in length, $\Delta L/L$, as the temperature is decreased for silver phosphosulphate glasses with compositions $(Ag_2SO_4)_{0.1}(AgPO_3)_{0.9}$, $(Ag_2SO_4)_{0.2}(AgPO_3)_{0.8}$, and $(Ag_2SO_4)_{0.3}(AgPO_3)_{0.7}$ each follow the same distinctive pattern (Fig. 10). From room temperature down to about 136 K, the length decreases linearly as the temperature is reduced. But at this temperature the linear thermal expansion coefficient β becomes negative for each of these glasses. The thermal expansions of the phosphosulphide $(Ag_2S)_x(AgPO_3)_{(1-x)}$ glasses (Fig. 11) and of

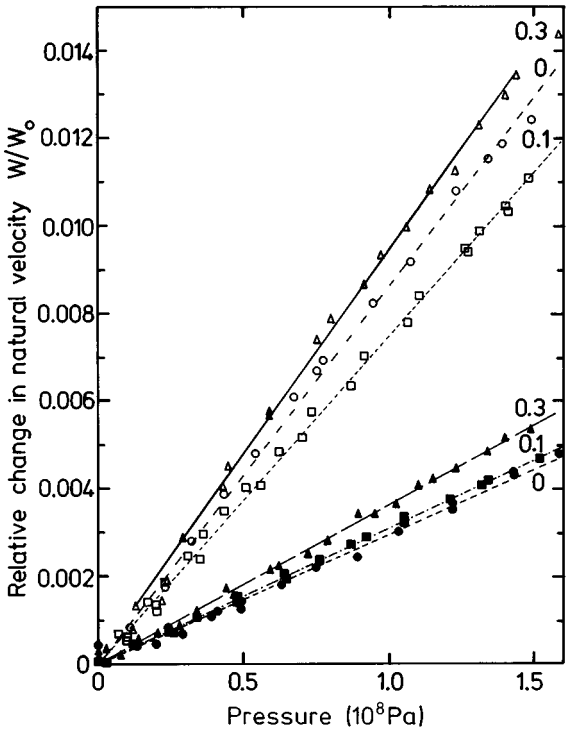

FIG. 8. Hydrostatic-pressure-induced relative change in the natural velocity of longitudinal (upper three plots) and shear (lower three plots) ultrasonic waves propagated in $Ag_2(SO_4)_x(AgPO_3)_{(1-x)}$ glasses.

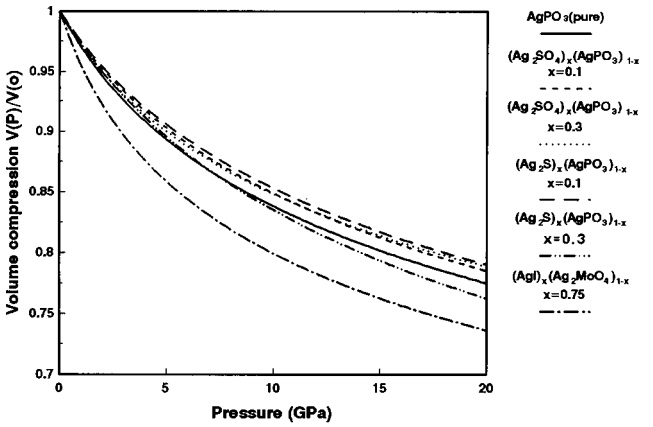

FIG. 9. Isothermal compressions $V(P)/V(0)$ of $(Ag_2SO_4)_x(AgPO_3)_{(1-x)}$, $(Ag_2S)_x(AgPO_3)_{(1-x)}$, and $(AgI)_{0.75}(Ag_2MoO_4)_{0.25}$ glasses at 293 K extrapolated to high pressure using the Murnaghan equation of state.

vitreous $AgPO_3$ (Fig. 12) show even more anomalous behavior. In these glasses $\Delta L/L$ also decreases with reducing temperature, although not in a linear fashion, down to about 150 K. At lower temperatures β becomes a large negative quantity. For $AgPO_3$ glass Bogue and Sladek[3] have reported similar thermal expansion behavior to that found here; from room temperature down to about 100 K, they observed that the thermal expansion coefficient was positive ($\sim+2.2\times10^{-5}$ K^{-1}): it passed through zero at about 160 K and then became negative (-2.0×10^{-5} K^{-1}) at lower temperatures.

In the quasiharmonic approximation the thermal Grüneisen parameter γ^{th}, a widely used measure of net vibrational anharmonicity, is related to the volume thermal expansion β_V and specific heat C by

$$\gamma^{\text{th}}=\frac{\beta_V V B^S}{C_p}=\frac{\beta_V V B^T}{C_v}, \tag{14}$$

where B^S and B^T are the isoentropic and isothermal bulk moduli, respectively. The thermal Grüneisen parameter γ^{th} is the weighted average of all the individual mode (i) Grüneisen parameters γ_i:

$$\gamma^{\text{th}}=\sum_i C_i\gamma_i \Big/ \sum_i C_i . \tag{15}$$

For a glass, measurements of the hydrostatic pressure derivatives of the elastic stiffness tensor components can be used to determine the Grüneisen parameters of the acoustic modes in the long-wavelength limit and so enable the effects of these modes to be separated from those of higher-energy excitations. As temperature is reduced, the higher-energy excitations would be expected to freeze out first and their contributions should decrease so that the long-wavelength acoustic phonons should play an increasingly important role. In general, a negative thermal expansion would be expected to result from the overriding cancellation of effects from excitations having negative Gruneisen parameters. However, for each of the $(Ag_2SO_4)_x(AgPO_3)_{(1-x)}$, $(Ag_2S)_x(AgPO_3)_{(1-x)}$, and pure $AgPO_3$ glasses, positive values for the acoustic mode Grüneisen parameters γ_L and γ_S have been obtained at room temperature, a feature which suggests that it is not

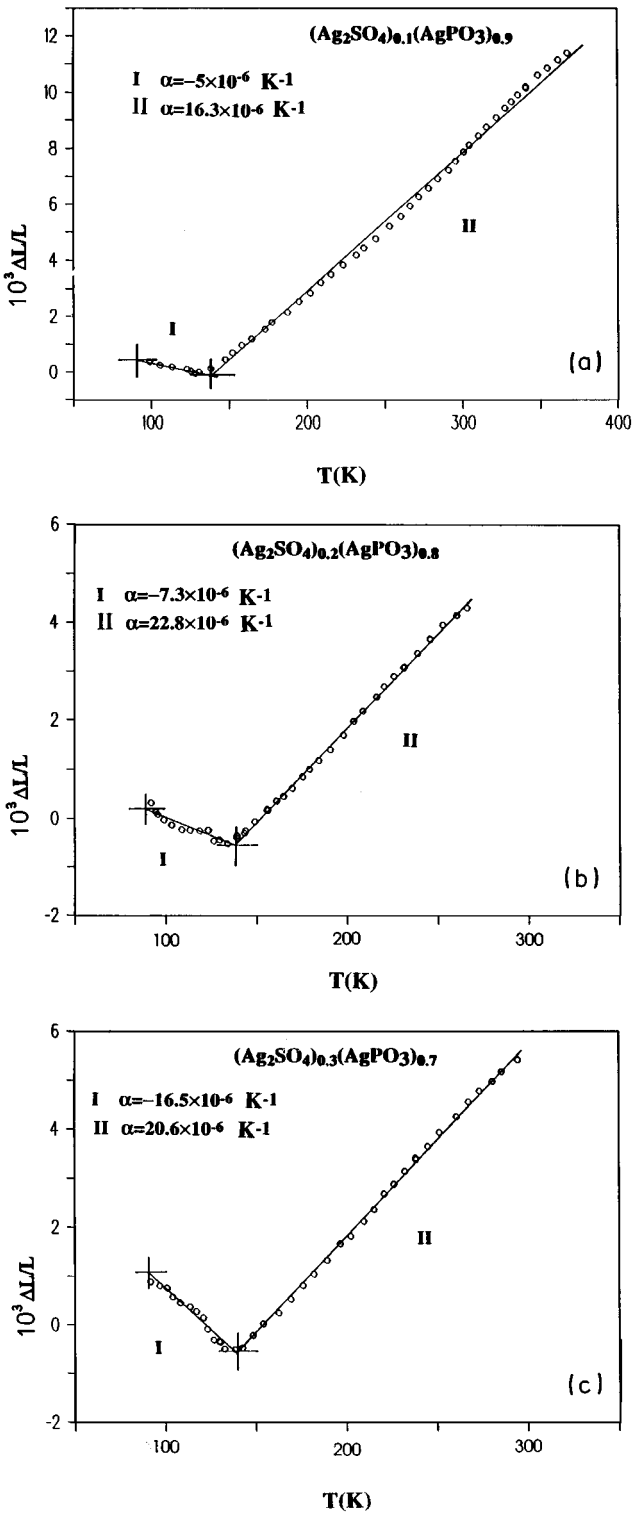

FIG. 10. Temperature dependence of the linear coefficient α of thermal expansion of (a) $(Ag_2SO_4)_{0.1}(AgPO_3)_{0.9}$, (b) $(Ag_2SO_4)_{0.2}(AgPO_3)_{0.8}$, and (c) $(Ag_2SO_4)_{0.3}(AgPO_3)_{0.7}$ glasses.

likely that these modes are responsible for the negative thermal expansion at lower temperatures (Figs. 10–12). Thus, although the thermal expansion data suggest that the net vibrational anharmonicity of each of the superionic glasses in the $(Ag_2SO_4)_x(AgPO_3)_{(1-x)}$ and $(Ag_2S)_x(AgPO_3)_{(1-x)}$ series and vitreous $AgPO_3$ becomes extremely anomalous at low temperature, it is not clear which excitations are responsible.

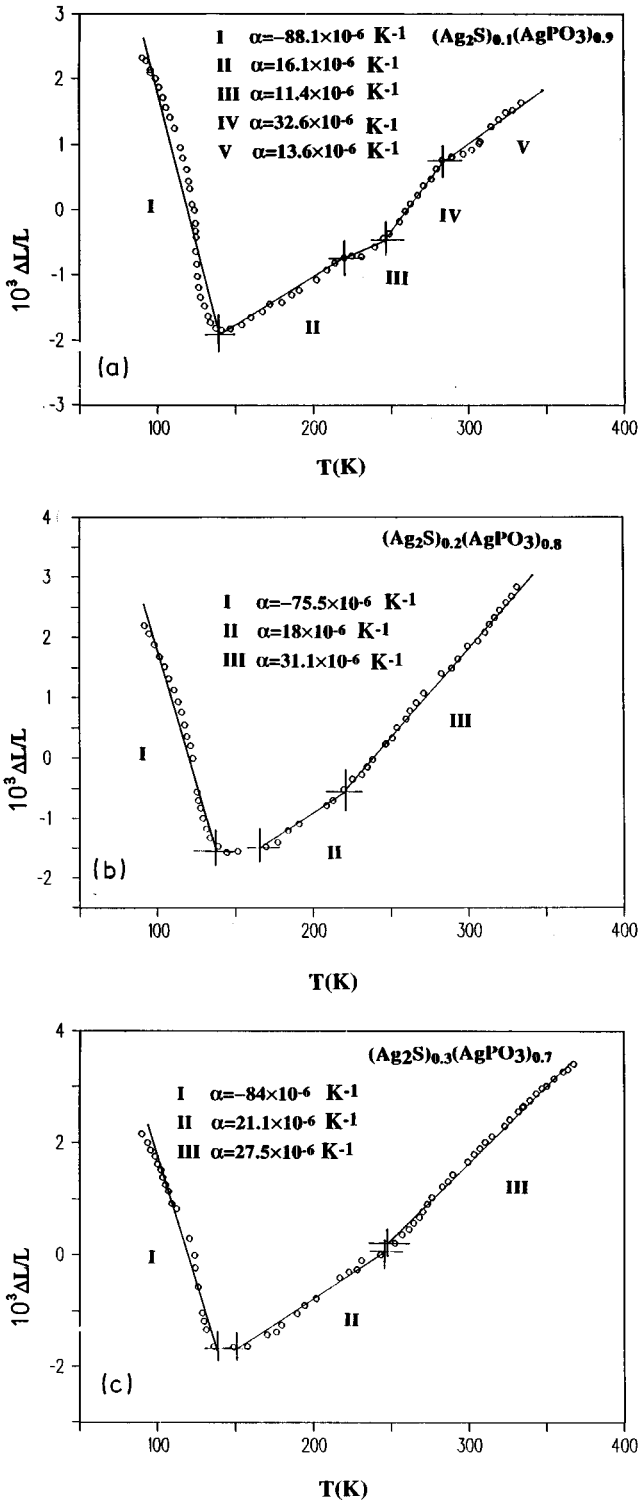

FIG. 11. Temperature dependence of the linear coefficient α of thermal expansion of (a) $(Ag_2S)_{0.1}(AgPO_3)_{0.9}$, (b) $(Ag_2S)_{0.2}(AgPO_3)_{0.8}$, and (c) $(Ag_2S)_{0.3}(AgPO_3)_{0.7}$ glasses.

One possible source is the topological disorder in glasses, which introduces the supplementary degrees of freedom, giving rise to the ''universal'' anomalies in thermal, acoustic, optical, and dielectric properties.[29,31–33] In the absence of specific-heat data, it is not possible to calculate the thermal Grüneisen parameter, which would be instructive.

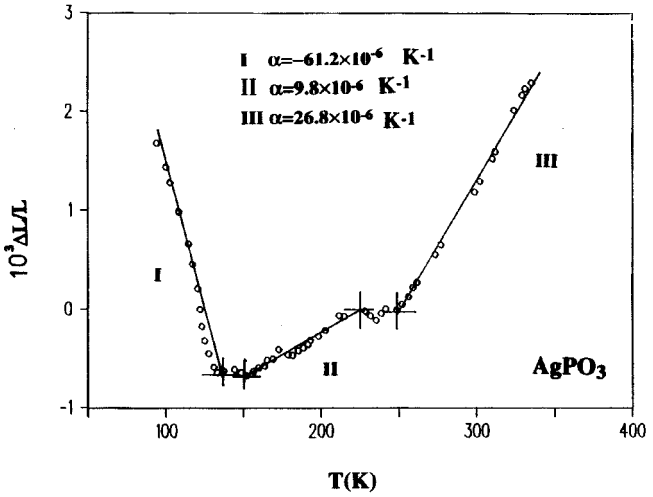

FIG. 12. Temperature dependence of the linear coefficient α of thermal expansion of $AgPO_3$ glass.

VII. ELASTIC STIFFNESS AND FRACTAL BOND CONNECTIVITY

The ultrasonic wave velocities and the elastic properties of a wide range of superionic glasses from different phosphate, borate, and molybdate systems vary widely from glass to glass (Tables II and III). For example, the bulk modulus covers the range from 4.66×10^{10} N m^{-2} for vitreous $(Ag_2O)_{0.33}(B_2O_3)_{(0.67)}$ to only 1.82×10^{10} N m^{-2} for the molybdate glass $(AgI)_{0.75}(Ag_2MoO_4)_{0.25}$ (Table II): The latter material is nearly 3 times as easy to compress as the former. This wide variation in behavior also extends to the effect of pressure on the elastic moduli and related properties (Table II) and must have its origin in differences in structure and binding forces between the glasses. An instructive parameter relating the elastic properties of glasses to their network structure is fractal bond connectivity. Considering a two-dimensional (2D) Sierpinski gasket as the fractal object in a study of the critical behavior of a random, d-dimensional, isotropic, elastic medium, Bergman and Kantor[8] have shown that the effective fractal dimensionality of an inhomogeneous random mixture of fluid and a solid backbone at threshold is given by

$$d=4C_{44}/B. \tag{16}$$

The fractal bond connectivity d should vary from $d=3$ for 3D networks of tetrahedral coordination polyhedra to $d=2$ for 2D structures and to $d=1$ for 1D chains, enabling Bogue and Sladek[3] to associate it with the connectivity of glass networks; we follow their suggestion here since this approach provides useful insight into the nature of the skeletal configuration. Whether glasses can be considered to have a fractal character has been difficult to establish. In fact, most testing of fractal models for amorphous solids has been carried out on suitably prepared aerogels.[34] A value of $d=1$ would be expected for a glass having a nearly one-dimensional structure $d=2$ for a two-dimensional network: Values of this order are found in quasi-2D glasses such as As_2S_3 and As_2Se_3 (Table IV) and in many borate glasses (Table III). In the tetrahedrally coordinated network glasses such as SiO_2, d is around 3 (Table IV). The fractal

TABLE III. Elastic properties and bond connectivities of borate glasses at room temperature calculated from published ultrasonic wave velocity data: $(Ag_2O)_y(B_2O_3)_{(1-y)}$ (Refs. 2, 35), $(Li_2O)_y(B_2O_3)_{(1-y)}$ (Ref. 36), $(K_2O)_y(B_2O_3)_{(1-y)}$ (Ref. 37), and $(Na_2O)_y(B_2O_3)_{(1-y)}$ (Ref. 38).

	Mole fraction y	Density (kg m^{-3})	Ultrasonic wave velocity (m s^{-1})		Elastic moduli ($\times 10^{10}$ N m^{-2})			Bond connectivity $4C_{44}/B$
			V_1	V_S	C_{11}	C_{44}	B	d
$(Ag_2O)_y(B_2O_3)_{(1-y)}$								
	0.00	4030	4232	2181	7.218	1.917	4.662	1.64
	0.10	4270	4079	2078	7.105	1.844	4.646	1.59
	0.20	4380	3895	2049	6.645	1.839	4.193	1.75
	0.40	4660	3509	1819	5.738	1.542	3.682	1.68
	0.50	4750	3238	1679	4.980	1.339	3.195	1.68
	0.60	4840	3011	1603	4.388	1.244	2.730	1.82
	0.00	3280	4191	2236	5.761	1.640	3.575	1.84
	0.20	3360	3911	2141	5.139	1.540	3.086	2.00
	0.30	3550	3868	2045	5.311	1.485	3.332	1.78
	0.40	3650	3640	1925	4.836	1.353	3.033	1.78
	0.30	5420	3367	1606	6.144	1.398	3.281	1.31
	0.40	5550	3134	1524	5.451	1.289	3.732	1.38
	0.50	5680	2843	1314	4.591	0.981	3.283	1.19
	0.60	5760	2545	1168	3.731	0.786	2.683	1.17
	0.70	5820	2276	1030	3.015	0.617	2.192	1.13
$(Li_2O)_y(B_2O_3)_{(1-y)}$	0.00	1800	3470	1910	2.167	0.657	1.292	2.03
	0.11	1980	4800	2620	4.562	1.359	2.750	1.98
	0.25	2100	5670	3160	6.751	2.097	3.955	2.12
	0.50	2050	6920	3970	9.817	3.231	5.509	2.35
	0.70	2300	7110	4070	11.627	3.810	6.547	2.33
$(K_2O)_y(B_2O_3)_{(1-y)}$	0.10	2050	4332	2375	3.847	1.156	2.305	2.01
	0.20	2138	4560	2480	4.446	1.315	2.692	1.95
	0.30	2282	4962	2719	5.619	1.687	3.369	2.00
	0.34	2306	4914	2653	5.568	1.623	3.404	1.91
$(Nd_2O)_y(B_2O_3)_{(1-y)}$	0.10	2047	4564	2520	4.264	1.300	2.531	2.05
	0.20	2186	5197	2857	5.904	1.784	3.525	2.02
	0.30	2340	5721	3204	7.659	2.402	4.456	2.16
	0.36	2386	5744	3196	7.872	2.437	4.623	2.11

bond connectivity for $(AgI)_x(AgPO_3)_{(1-x)}$ glasses was found to decrease monotonically with increasing AgI concentration from the value of 1.10 in the pure $AgPO_3$ glass to 0.88 at $x=0.46$.[3] The value of 1.10 found for a pure $AgPO_3$ metaphosphate glass sample is consistent with a structure comprised of chains of PO_4 tetrahedra which are very weakly cross-linked. The decrease of d below unity implies breaking of the phosphate chains, when AgI is included. The present values found for d decrease somewhat from 1.22 for the pure $AgPO_3$ glass to below unity for $(Ag_2SO_4)_x(AgPO_3)_{(1-x)}$ ($d=0.96$ and 0.91 for $x=0.1$ and 0.3, respectively), but remain above unity for $(Ag_2S)_x(AgPO_3)_{(1-x)}$ ($d=1.11$ and 1.10 for $x=0.1$ and 0.3, respectively). This implies some cross-linking between the phosphate chains in these glasses. NMR studies of $(Ag_2SO_4)_x(AgPO_3)_{(1-x)}$ glasses suggest a network-modifying effect by which metaphosphate chains are converted to "end units" with a bridging sulphate;[7] a reduction of d to less than unity with Ag_2SO_4 addition to the phosphate glass is consistent with such a modifying effect. By contrast, for the $(Ag_2S)_x(AgPO_3)_{(1-x)}$ glasses the fractal bond connectivity remains greater than unity after addition of Ag_2S. A NMR study has shown that Ag_2S is less effective than Ag_2SO_4 in modifying polyphosphate chains into end units.[6] That the fractal bond connectivity is greater than unity is in qualitative agreement with a smaller induced reduction in chain length and cross-linking by Ag_2S.

In contrast to the essentially one-dimensional chain structure of the silver metaphosphate glasses, borate glasses are considered to be based on two-dimensional configurations of the planar (BO_3) triangular unit, and indeed a wide range of borate glasses is found to have a fractal dimension d nearer 2 (Table III). In the case of the borate glasses of the type $(AgI)_x\{(Ag_2O)_y(B_2O_3)_{(1-y)}\}_{(1-x)}$ with $y=0.2$, 0.33, and 0.5,[1,17] the effect of AgI doping is nonmonotonic, an increase in y, the mole fraction of Ag_2O, leading to a reduction of d, consistent with the breaking of B-O-B bridges and the reduction of network connectivity. An important difference between the borate-based glasses $(Ag_2O)_y(B_2O_3)_{(1-y)}$ and

TABLE IV. Elastic properties and comparison between the fractal bond connectivity (d) of glasses. References indicate the sources of the bulk (B) and shear (C_{44}) moduli (units 10^{10} Pa).

Glass	Reference	B	C_{44}	Fractal bond connectivity d
Fused SiO_2	39	3.63	3.15	3.47
Vycor	40	2.65	2.27	3.43
$(K_2O)(SiO_2)_3$	41	2.83	2.41	3.41
Pyrex	42	4.18	2.79	2.67
Sodium borosilicate	43	3.40	2.12	2.49
$(Fe_2O_3)_{0.38}(P_2O_5)_{0.62}$	44	4.30	2.69	2.50
$(V_2O_5)_{0.45}(P_2O_5)_{0.55}$	45	3.84	2.18	2.27
$(Sm_2O_3)_{0.25}(P_2O_5)_{0.75}$	46	3.91	2.38	2.44
$(ZnO)_{0.535}(P_2O_5)_{0.465}$	47	2.73	1.59	2.33
$(MoO_3)_{0.35}(P_2O_5)_{0.65}$	48	2.19	1.68	3.07
$(CuO)_{0.54}(P_2O_5)_{0.46}$	45	3.97	2.47	2.49
As	49	1.75	0.928	2.12
Se	50	0.94	0.369	1.57
As_2Se_3	51	1.36	0.673	1.98
As_2S_3	51	1.20	0.566	1.89
$Pd_{0.40}Ni_{0.40}P_{0.20}$	52	18.5	3.86	0.83

$(AgI)_x\{(Ag_2O)_y(B_2O_3)_{(1-y)}\}_{(1-x)}$ (Ref. 2) and the phosphate $(AgI)_x(AgPO_3)_{(1-x)}$ (Ref. 3) glasses is that for the borates the shear mode softens under pressure,[2] but in contrast the vibrational anharmonicity of the long-wavelength shear modes propagated in $(AgI)_x(AgPO_3)_{(1-x)}$ glasses is normal.[3] Another marked difference in vibrational mode anharmonicities is that the acoustic mode Grüneisen parameters γ_L and γ_S are substantially larger for the phosphates than for the borates (Table I). The shear mode softening in the borates results from the open two-dimensional structure, which allows bending vibrations involving bridging oxygen atoms. The marked differences between the acoustic mode vibrational anharmonicities between the phosphate and borate glasses is associated with the essentially one-dimensional nature of the former and two-dimensional structure of the latter.

Finally, it is interesting to place the elastic and nonlinear acoustic behavior of the phosphate-based superionic glasses in context with those of other metaphosphate glasses $M(PO_3)_x$, where M is a metal cation of valence x. In general, such materials comprise a network of PO_4 tetrahedra, each fourfold-coordinated phosphorus having one doubly bonded and a singly bonded oxygen and two bridging oxygens to neighboring tetrahedra. The polyphosphate skeletal groups are interconnected by rather weaker ionic bonds to the metal cations. The fractal bond connectivity determined (Table IV) for the phosphate glasses modified with cations having a valency greater than unity range between 2.27 and 3.07. When the cation valence is greater than unity, more cross-linkage occurs and so phosphate glasses modified with cations such as Zn^{2+}, Cu^{2+}, Fe^{3+}, Sm^{3+}, V^{5+}, and Mo^{6+}, which have compositions in the vicinity of the metaphosphate composition, have a three-dimensional phosphate skeleton. This is quite different from that of the silver-phosphate-based superionic glasses, which are comprised of the one-dimensional polyphosphate chains which dominates the elastic and nonlinear acoustic properties of the superionic silver-phosphate-based glasses.

VIII. CONCLUSIONS

(1) The attenuation and velocity of ultrasonic waves have been measured in superionic silver phosphosulphate $(Ag_2SO_4)_x(AgPO_3)_{(1-x)}$ and phosphosulphide $(Ag_2S)_x(AgPO_3)_{(1-x)}$ glasses as a function of temperature between 1.5 and 300 K. In general, the temperature dependences of the acoustic properties in the MHz frequency region indicates that the Ag_2S and Ag_2SO_4 dopant salts play a different role in the structure-dependent properties of these superionic glasses.[2,3] The broad high-temperature relaxation loss peak characteristic of glasses has been used to determine the relaxation parameters.

(2) For the $(Ag_2SO_4)_{0.3}(AgPO_3)_{0.7}$ and $(Ag_2S)_{0.3}(AgPO_3)_{0.7}$ glasses below 100 K, there is a contribution to ultrasonic velocity, in addition to those arising from the relaxation effects and the anharmonic interactions, which follows a linear temperature dependence. This is the behavior predicted by the SPM for a relaxation mechanism involving soft single-well harmonic oscillators (HO's) which interact with the ultrasonic deformation field by a modulation of the interlevel spacing. The soft HO relaxation contribution to the ultrasonic velocity temperature dependences of silver-phosphate-based and lanthanide metaphosphate glasses, which are quite different in structure, has a similar magnitude, in accordance with the suggestion that the SPM should be universally applicable to glasses.

(3) Velocities of ultrasonic waves propagated in the molybdate $(AgI)_{0.75}(Ag_2MoO_4)_{0.25}$ glass are much slower, and the elastic stiffnesses C_{11} and C_{44} and the bulk modulus B_0^S are correspondingly much smaller than those in the silver phosphates. The silver-molybdate-based glass has a much larger compression than those found for the stiffer phosphates. The binding forces in the molybdate are much weaker than those in the phosphate glasses.

(4) The velocities of longitudinal and shear ultrasonic waves propagated in the $(Ag_2S)_x(AgPO_3)_{(1-x)}$, $(Ag_2SO_4)_x(AgPO_3)_{(1-x)}$, and $(AgI)_{0.75}(Ag_2MoO_4)_{0.25}$ glasses are linearly dependent upon hydrostatic pressure. The pressure derivatives for each of these glasses are positive with $(\partial C_{11}^S/\partial P)_{T,P=0}$ being much larger than $(\partial C_{44}^S/\partial P)_{T,P=0}$.

(5) For the phosphate-based superionic glasses, the long-wavelength shear mode softens under pressure in contrast to the stiffening observed for the corresponding borates. The long-wavelength acoustic mode Grüneisen parameters γ_L and γ_S are substantially larger for the phosphates than for the borates. The shear mode γ_S is negative for the $(Ag_2O)_y(B_2O_3)_{(1-y)}$ and $(AgI)_x\{(Ag_2O)_y(B_2O_3)_{(1-y)}\}_{(1-x)}$ glasses. For the phosphate glasses the acoustic mode frequencies increase in the usual manner under pressure, the effect being larger for the volume-dependent longitudinal modes.

(6) The linear thermal expansion coefficient β becomes anomalously negative at lower temperatures for each of the $(Ag_2SO_4)_x(AgPO_3)_{(1-x)}$ and $(Ag_2S)_x(AgPO_3)_{(1-x)}$ glasses.

(7) In contrast to the essentially one-dimensional chain structure of the silver metaphosphate glasses, the borate glasses are based on two-dimensional configurations of the

planar (BO_3) triangular unit: A wide range of borate glasses has a fractal bond connectivity nearer to 2. The differences between the effects of pressure on the elastic behavior and vibrational anharmonicity of the long-wavelength acoustic modes of the two types of glass have been associated with these structural differences.

ACKNOWLEDGMENTS

We are grateful to Dr. D. P. Almond for providing a silver molybdate glass specimen, to Dr. A. Magistris for preparing the silver sulphide and silver sulphate phosphate glasses, to E. F. Lambson for experimental assistance, and to Dr. H. B. Senin for many valuable discussions.

*On sabbatical leave from Faculty of Applied Science, University of Central Queensland, Rockhampton Campus, Q4702, Australia.

[1] G. Carini, M. Cutroni, M. Federico, and G. Tripodo, Phys. Rev. B **37**, 7021 (1988).
[2] G. A. Saunders, H. A. A. Sidek, J. D. Comins, G. Carini, and M. Federico, Philos. Mag. B **56**, 1 (1987).
[3] R. Bogue and R. J. Sladek, Phys. Rev. B **42**, 5280 (1990).
[4] J. Gombeau and H. Z. Keller, Inorg. Chem. **272**, 303 (1953).
[5] F. L. Galeener, G. Lucovsky, and J. C. Mikkelsen, Phys. Rev. B **22**, 3983 (1980).
[6] M. Cutroni, A. Magistris, and M. Villa, Solid State Ion. **53-56**, 1232 (1992), and references therein.
[7] S. Scotti, M. Villa, P. Mustarelli, and M. Cutroni, Solid State Ion. **53-56**, 1237 (1992).
[8] D. J. Bergman and Y. Kantor, Phys. Rev. Lett. **53**, 511 (1984).
[9] R. C. Zeller and R. O. Pohl, Phys. Rev. B **4**, 2029 (1971).
[10] W. A. Phillips, J. Low Temp. Phys. **7**, 351 (1972).
[11] A. Avogadro, S. Aldrovani, and F. Borsa, Phys. Rev. B **33**, 5637 (1986).
[12] S. Alexander and R. Orbach, J. Phys. (Paris) **43**, L625 (1982).
[13] R. Orbach, Science **231**, 814 (1986).
[14] V. G. Karpov, M. I. Klinger, and F. N. Ignatiev, Zh. Eksp. Teor. Fiz. **84**, 760 (1983) [Sov. Phys. JETP **57**, 439 (1983)].
[15] V. G. Karpov and D. A. Parschin, Pis'ma Zh. Eksp. Teor. Fiz. **38**, 536 (1983) [Sov. Phys. JETP Lett. **38**, 648 (1983)].
[16] G. Carini, G. D'Angelo, G. Tripodo, and G. A. Saunders, Nuovo Cimento D **16**, 1277 (1994).
[17] G. Carini, G. D'Angelo, M. Federico, G. Tripodo, G. A. Saunders, and H. B. Senin, Phys. Rev. B **50**, 2858 (1994).
[18] U. Buchenau, Yu. M. Galperin, V. L. Gurevich, and H. R. Schober, Phys. Rev. B **43**, 5039 (1991).
[19] U. Buchenau, Yu. M. Galperin, V. L. Gurevich, D. A. Parschin, M. A. Ramos, and H. R. Schober, Phys. Rev. B **46**, 2798 (1992).
[20] D. A. Parschin, Phys. Rev. B **49**, 9400 (1994).
[21] D. P. Almond, G. K. Duncan, and A. R. West, J. Non-Cryst. Solids **74**, 285 (1985).
[22] E. P. J. Papadakis, Acoust. Soc. Am. **42**, 1045 (1967).
[23] R. N. Thurston and K. Brugger, Phys. Rev. **133**, A1604 (1964).
[24] J. Jäckle, Z. Phys. **257**, 212 (1972).
[25] O. L. Anderson and H. E. Bömmel, J. Am. Ceram. Soc. **38**, 125 (1955).
[26] M. Cutroni, A. Mandanici, A. Piccolo, P. Mustarelli, C. Fanggao, and G. A. Saunders, Philos. Mag. (to be published).
[27] T. N. Slater and R. J. Sladek, Phys. Rev. B **18**, 5842 (1978).
[28] J. A. Garber and A. V. Granato, Phys. Rev. B **11**, 3990 (1975).
[29] S. Hunklinger and M. V. Schickfus, in *Amorphous Solids*, edited by W. A. Phillips, Topics in Current Physics Vol. 24 (Springer-Verlag, Berlin, 1981), p. 81.
[30] F. D. Murnaghan, Proc. Natl. Acad. Sci. **30**, 244 (1944).
[31] R. O. Pohl, in *Amorphous Solids*, edited by W. A. Phillips, Topics in Current Physics Vol. 24 (Springer-Verlag, Berlin, 1981), p. 27.
[32] J. Jäckle, in *Amorphous Solids*, edited by W. A. Phillips, Topics in Current Physics Vol. 24 (Springer-Verlag, Berlin, 1981), p. 135.
[33] W. A. Phillips, in *Phonons '89*, edited by S. Hunklinger, W. Ludwig, and G. Weiss (World Scientific, Singapore, 1989), p. 367.
[34] R. Vacher, T. Woignier, J. Pelous, and E. Courtens, Phys. Rev. B **37**, 6500 (1988).
[35] G. Carini., M. Cutroni, M. Federico, and G. Tripodo, Phys. Rev. B **32**, 8264 (1985).
[36] M. Devaud, J-Y. Prieur, and D. Wallace (unpublished).
[37] M. Kodama, J. Non-Cryst. Solids **127**, 65 (1991).
[38] M. Kodama, J. Mater. Sci. **26**, 4048 (1991).
[39] E. H. Bogardus, J. Appl. Phys. **36**, 2504 (1965).
[40] M. H. Manghnani and W. M. Benzing, J. Phys. Chem. Solids **30**, 2241 (1969).
[41] J. C. Thompson and K. E. Bailey, J. Non-Cryst. Solids **27**, 161 (1978).
[42] D. S. Hughes and J. K. Kelly, Phys. Rev. **92**, 1145 (1953).
[43] C. A. Maynell, G. A. Saunders, and S. Scholes, J. Non-Cryst. Solids **12**, 271 (1973).
[44] M. P. Brassington, A. J. Miller, J. Pelzl, and G. A. Saunders, J. Non-Cryst. Solids **44**, 157 (1981).
[45] J. M. Farley and G. A. Saunders, Phys. Status Solidi A **28**, 199 (1975).
[46] A. Mierzejewski, G. A. Saunders, H. A. A. Sidek, and B. Bridge, J. Non-Cryst. Solids **104**, 323 (1988).
[47] A. A. Higazy, B. Bridge, A. Hussein, and M. A. Ewaida, J. Acoust. Soc. Am **86**, 1453 (1989).
[48] J. D. Comins, J. E. Macdonald, E. F. Lambson, G. A. Saunders, A. J. Rowsell, and B. Bridge, J. Mater. Sci. **22**, 2113 (1987).
[49] M. P. Brassington, W. A. Lambson, A. J. Miller, G. A. Saunders, and Y. K. Yogurtçu, Philos. Mag. B **42**, 127 (1980).
[50] P. J. Ford, G. A. Saunders, E. F. Lambson, and G. Carini, Philos. Mag. Lett. **57**, 201 (1988).
[51] M. P. Brassington, A. J. Miller, and G. A. Saunders, Philos. Mag. B **43**, 1049 (1981).
[52] E. F. Lambson, W. A. Lambson, J. E. Macdonald, M. R. J. Gibbs, G. A. Saunders, and D. Turnbull, Phys. Rev. B **33**, 2380 (1986).